Effect of the depolarization field on coherent optical properties in semiconductor quantum dots

Yasuyoshi Mitsumori,* Shunta Watanabe, Kenta Asakura, Keisuke Seki, and Keiichi Edamatsu
Research Institute of Electrical Communication, Tohoku University, Sendai 980-8577, Japan

Kouichi Akahane and Naokatsu Yamamoto
National Institute of Information and Communications Technology, Tokyo 184-8795, Japan

(Received 28 August 2017; revised manuscript received 22 April 2018; published 6 June 2018)

We study the photon echo spectrum of self-assembled semiconductor quantum dots using femtosecond light pulses. The spectrum shape changes from a single-peaked to a double-peaked structure as the time delay between the two excitation pulses is increased. The spectrum change is reproduced by numerical calculations, which include the depolarization field induced by the biexciton-exciton transition as well as the conventional local-field effect for the exciton–ground-state transition in a quantum dot. Our findings suggest that various optical transitions in tightly localized systems generate a depolarization field, which renormalizes the resonant frequency with a change in the polarization itself, leading to unique optical properties.

DOI: 10.1103/PhysRevB.97.235305

I. INTRODUCTION

When a static electric field is applied to a dielectric particle, charges are induced at the surface, together with the creation of microscopic polarization densities in the particle, as shown in Fig. 1(a). The induced charges provide a depolarization field and correct the field inside the particle. This is known as a local field [1]. This physical concept is true in the case of an oscillating electric field, when the particle is much smaller than the wavelength of the field because the wave vector can be neglected and the interaction between the electric field and a matter can be treated as quasistatic. In a semiconductor quantum dot (QD), the excitonic polarization is tightly localized, and the size is much smaller than the resonant wavelength [2]. Therefore, the concept can be applied to the optical properties of a QD. If we assume that the single excitonic polarization is uniformly distributed in a QD, charges are optically induced at the surface, as for a dielectric particle. The depolarization field provided by the charges interacts with the polarization densities distributed in the QD. Therefore, the exciton resonant frequency is renormalized with a change in the polarization itself, referred to as the local-field effect (LFE) in the QD [3–7]. Recently, we demonstrated that the LFE significantly affected the optical response of a QD ensemble, using picosecond light pulses [6,7]. The narrow spectral bandwidth of picosecond pulses selectively drives only exciton resonances in the QD ensemble. However, in a QD, many carriers, as well as a single exciton, are easily populated by optical excitations. In particular, the biexciton can be coherently created by femtosecond light pulses with a spectral bandwidth wider than the biexciton binding energy [8–10]. In higher-dimensional semiconductors, coherent effects relating to both the LFE and the biexciton have been well analyzed [11–13] and optical properties of the biexciton connecting with the LFE have been discussed [14–16]. However, for QD systems, neither observation of the LFE including the biexciton nor theoretical analysis has been reported yet.

In this paper, we report the effect of the depolarization field induced by the biexciton-exciton (B-X) transition, as well as the exciton–ground-state (X-G) transition, in QDs by measuring the photon echo (PE) spectrum using femtosecond light pulses. The PE spectrum shows a strong dependence on the time delay τ of the two excitation pulses. The dependence can be reproduced by introducing a depolarization field induced by the B-X transition to conventional LFE theories in a QD [3–5]. We also discuss the relevance to the electron-hole exchange interaction, which is described by the same Hamiltonian for the LFE, from an experimental viewpoint. Our findings show that the depolarization field strongly affects the optical properties of various optical transitions in tightly localized systems.

II. SAMPLE AND EXPERIMENTAL METHODS

The sample in this paper was a single layer of self-assembled undoped $In_{0.4}Al_{0.1}Ga_{0.5}As$ QDs embedded in $Al_{0.17}Ga_{0.83}As$ barrier layers, which were fabricated by molecular-beam epitaxy on a GaAs (311)B substrate. The QDs had a dome shape with a diameter at the bottom of the QD $d = 50$–70 nm and a height $h = 4$–7 nm, and their density was $\sim 1.1 \times 10^{10}/\mathrm{cm}^2$, as shown by an atomic force microscope image of the sample in Fig. 1(b). Figure 1(c) shows the photoluminescence (PL) spectrum at 3.5 K. The PL peak was located at 1.565 eV, and the inhomogeneous broadening was ~40 meV. In order to confirm the biexciton formation, we measured the micro PL spectrum from the sample through an aperture with a diameter of 400 nm. The aperture was fabricated by electron-beam lithography and metal liftoff to open an aperture in an opaque 150-nm-thick Au layer deposited on the sample surface. As shown in Fig. 1(d), we could observe a single peak labeled by X in the spectrum at 1.610 eV when we excited the barrier layer located at 1.720 eV by a cw laser. With increasing excitation density P, an

*mitumori@riec.tohoku.ac.jp

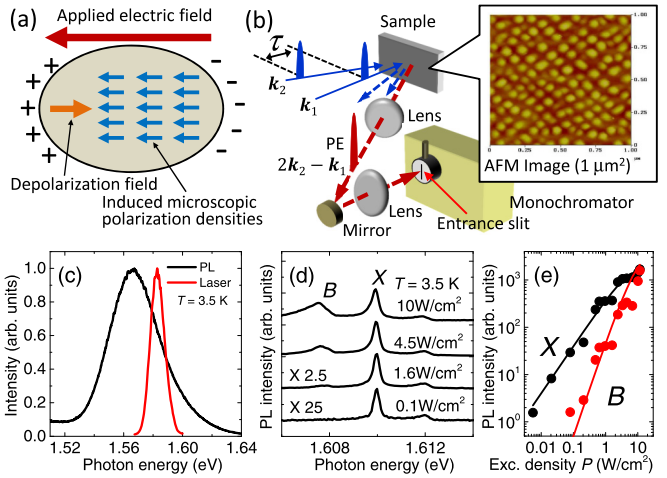

FIG. 1. (a) Illustration of a dielectric particle in a static electric field. (b) Schematic drawing of the experimental setup, and atomic force microscope image of the uncapped sample. (c) PL spectrum of the sample, together with the laser spectrum. (d) Dependence of the micro PL spectrum on P. (d) PL intensities for the peak X and B vs P.

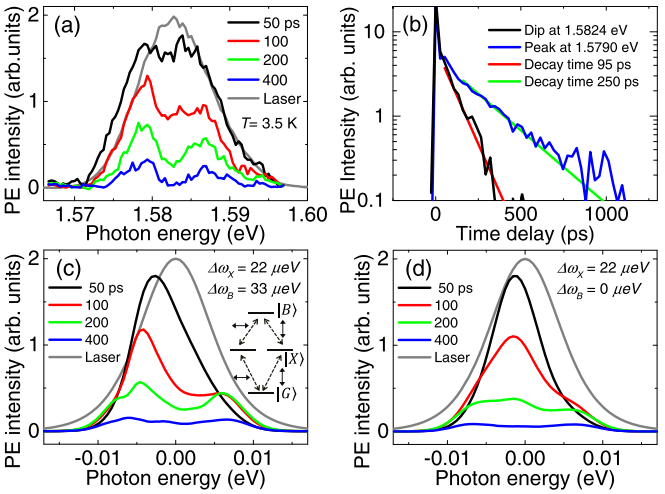

FIG. 2. (a) Dependence of the PE spectrum on τ. (b) PE responses at the dip (1.5824 eV) and the peak (1.5790 eV), together with the fitting curves. Dependences of the calculated PE spectrum on τ (c) with and (d) without the LFE of the biexcitons. Photon energy zero is given by the center of the laser spectrum. The selection rules for a biexciton system in the linear-polarization bases are illustrated in (c).

additional peak marked by B grows at an energy lower than X. In Fig. 1(e), we summarize each peak intensity as a function of P. The solid black and red lines represent the theoretical curves for the occupancy probabilities of the single ($N = 1$) and double particle ($N = 2$) states, respectively, when the number of the photogenerated carriers is assumed to be statistically distributed according to a Poisson distribution $\propto \alpha^N e^{-\alpha}/N!$, where α denotes the generation rate proportional to P [17]. The theoretical curves reproduce the PL intensities of X and B. Therefore, we attribute the X and B peaks to the exciton and the biexciton in the single QD. From the splitting energy, the biexciton binding energy can be estimated to be $\Delta E_B \sim 2.3$ meV. In InAs QDs, charged excitons have been infrequently observed even with an undoped sample at zero bias [10,18]. We measured the bias dependence of the micro PL spectrum of our sample with several QDs (data not shown), indicating that our QD system consists of neutral QDs at zero bias.

The experiment was carried out by measuring the PE spectrum. The light source was a mode-locked Ti:sapphire laser with a repetition rate of 76 MHz. The temporal duration and spectral width of the laser pulses were ~120 fs and ~10 meV, respectively. As shown in Fig. 1(c), the center of the laser spectrum was set to 1.5824 eV, which was slightly higher than the PL peak, in order to improve the signal-to-noise ratio by eliminating the strong scattered light from the band edge of the GaAs substrate. As shown in Fig. 1(b), the first and second pulses with wave vectors $\boldsymbol{k}_{1,2}$ were parallel linear polarized and focused on the same spot on the sample without the Au layer kept at 3.5 K in a cryostat. The beam spot had a Gaussian profile with a full width at half maximum of ~65 μm. The PE signal along $2\boldsymbol{k}_2 - \boldsymbol{k}_1$ in the reflection geometry was collected, and focused onto the entrance slit of a monochromator.

III. RESULTS AND DISCUSSION

Figure 2(a) shows the dependence of the PE spectrum on τ, together with the laser spectrum. The data were taken at the excitation intensities of the first pulse $I_1 \sim 35\,\mu\text{J/cm}^2$ per pulse and the second pulse $I_2 \sim 12\,\mu\text{J/cm}^2$ per pulse. The laser spectrum exhibits a Gaussian-like shape. On the other hand, the PE spectrum at $\tau = 50$ ps is slightly shifted to the lower-energy side of the center of the laser spectrum. Then, a peak appears at the lower energy while the higher-energy regime remains almost flat. With increasing τ, the spectrum splits into two peaks. Figure 2(b) shows the PE responses as a function of τ at the dip (1.5824 eV) and the peak (1.5790 eV) in the PE spectrum. In both scans, a large peak at zero time delay was observed. We attribute the peak to the GaAs substrate because the carriers in bulk crystals show a fast dephasing time [19]. Then, a slowly decaying signal was observed, which arises from the excited polarizations in the QDs. The decay times are estimated to be ~95 and ~250 ps for the dip and the peak, which give dephasing times $T_2 \sim 380$ ps and ~1 ns, respectively. From these T_2 values, the homogeneous linewidth is calculated to be 1.5–3.5 μeV, which is much narrower than the PL linewidth ~100 μeV of the single exciton in Fig. 1(c). We attribute the line broadening of the single PL to spectral diffusion, which has been demonstrated by single QD spectroscopies [20–24]. In the experiment using picosecond pulses, we estimate $T_2 \sim 2.5$ ns [6,7]. In general, the peak intensity of a femtosecond pulse is higher than that of a picosecond pulse even when the pulse energies are almost identical. Therefore, a femtosecond pulse generates many more incoherent carriers in the wetting layer through two-photon excitation than a picosecond pulse. The incoherent carriers are expected to give a fast decay time to the PE signal by disturbing the coherence of the polarizations in the QDs.

In order to confirm that the observed spectrum change is due to the LFE including the biexciton, we numerically calculate the PE spectrum. The optical effects of the biexcitons are generally described by a four-level system, which consists of the ground state $|G\rangle$ at the energy position of E_G, the

two single-exciton states $|X\rangle$ at E_X, and the biexciton state $|B\rangle$ at E_B, as illustrated in Fig. 2(c). In our experiment, the polarization directions of the two excitation pulses are parallel. Therefore, hereafter, we treat the three-level subsystem in a four-level system as a biexciton system for simplicity.

First, we introduce the B-X depolarization field to a three-level system. In the framework of the LFE in a QD [3,5], the Hamiltonian describing the interaction of the polarization at $\boldsymbol{r}$ and a depolarization field induced at $\boldsymbol{r}'$ in a QD is given by

$$H_{\rm dep} = -\iint_V d\boldsymbol{r}d\boldsymbol{r}'\hat{\boldsymbol{p}}(\boldsymbol{r})\cdot\nabla\nabla\frac{1}{4\pi\epsilon_h\mid\boldsymbol{r}-\boldsymbol{r}'\mid}\cdot\boldsymbol{p}(\boldsymbol{r}'), \quad (1)$$

where V and ϵ_h are the QD volume and the dielectric constant of the host material, respectively, $\hat{\boldsymbol{p}}(\boldsymbol{r})$ denotes a polarization operator at $\boldsymbol{r}$, and $\boldsymbol{p}(\boldsymbol{r}')$ represents a polarization density at $\boldsymbol{r}'$, which is treated as an averaged value of the operator, i.e., $\langle\hat{\boldsymbol{p}}(\boldsymbol{r}')\rangle$. $H_{\rm dep}$ is equivalent to the Hamiltonian for the electron-hole exchange interaction [25–29]. We discuss the relevance to the electron-hole exchange interaction, later. The spatial distribution of $\boldsymbol{p}(\boldsymbol{r}')$ is derived from the transition matrix element as $\boldsymbol{p}_X(\boldsymbol{r}') = \langle X|\hat{\boldsymbol{p}}^+(\boldsymbol{r}')|G\rangle$ for the exciton and $\boldsymbol{p}_B(\boldsymbol{r}') = \langle B|\hat{\boldsymbol{p}}^+(\boldsymbol{r}')|X\rangle$ for the biexciton using polarization operator $\hat{\boldsymbol{p}}^+(\boldsymbol{r}') = \hat{\boldsymbol{p}}^+\delta(\boldsymbol{r}-\boldsymbol{r}')$ at point $\boldsymbol{r}'$ [30], where $\hat{\boldsymbol{p}}^+$ represents a standard polarization operator [31,32]. In the strong confinement limit [31], the polarization densities are given by

$$\boldsymbol{p}_X(\boldsymbol{r}') = \boldsymbol{\mu}_X[\phi(\boldsymbol{r}',\boldsymbol{r}')]^*, \quad (2)$$

$$\boldsymbol{p}_B(\boldsymbol{r}') = \boldsymbol{\mu}_B\iint d\boldsymbol{r}_e d\boldsymbol{r}_h[\psi(\boldsymbol{r}_e,\boldsymbol{r}',\boldsymbol{r}_h,\boldsymbol{r}')]^*\phi(\boldsymbol{r}_e,\boldsymbol{r}_h), \quad (3)$$

where $\phi(\boldsymbol{r}_e,\boldsymbol{r}_h)$ and $\psi(\boldsymbol{r}_e,\boldsymbol{r}'_e,\boldsymbol{r}_h,\boldsymbol{r}'_h)$ denote the envelope functions of the exciton and the biexciton, and $\boldsymbol{\mu}_{B,X}$ represent the dipole moments for the B-X and X-G transitions, respectively. Without the Coulomb interaction between the carriers, as a first-order approximation in the strong confinement limit, the optically excited wave functions of the electrons and the holes are given by the same single-particle wave function $\zeta(\boldsymbol{r})$ [31]. Here, we focus on the lowest state for simplicity. ϕ and ψ are simply written by products of $\zeta(\boldsymbol{r})$ as one- and two-electron-hole pair states, i.e., $\phi = \zeta(\boldsymbol{r}_e)\zeta(\boldsymbol{r}_h)$ and $\psi = \zeta(\boldsymbol{r}_e)\zeta(\boldsymbol{r}'_e)\zeta(\boldsymbol{r}_h)\zeta(\boldsymbol{r}'_h)$. Therefore, $\boldsymbol{p}_X(\boldsymbol{r}')$ and $\boldsymbol{p}_B(\boldsymbol{r}')$ have the same form as $\zeta(\boldsymbol{r}')^2$ within the strong confinement limit, and the polarization operator at $\boldsymbol{r}$ including a biexciton can be written as

$$\hat{\boldsymbol{p}}(\boldsymbol{r}) = \zeta(\boldsymbol{r})^2(\boldsymbol{\mu}_X|X\rangle\langle G| + \boldsymbol{\mu}_B|B\rangle\langle X|) + \text{H.c.} \quad (4)$$

Consequently, $H_{\rm dep}$ for the three-level system in a QD is described as

$$H_{\rm dep} = \frac{N_{xx}}{\epsilon_h V}(\mu_X|X\rangle\langle G| + \mu_B|B\rangle\langle X| + \text{H.c.}) \times(\mu_X\langle|X\rangle\langle G|\rangle + \mu_B\langle|B\rangle\langle X|\rangle + \text{c.c.}), \quad (5)$$

when the oscillation directions of the polarization and the excitation external field are along the x axis. Here, N_{xx} represents a depolarization tensor, which depends on the shape of the polarization, and is calculated as

$$N_{xx} = -\frac{V}{4\pi}\iint_V d\boldsymbol{r}d\boldsymbol{r}'\zeta(\boldsymbol{r})^2\zeta(\boldsymbol{r}')^2\frac{\partial^2}{\partial x^2}\frac{1}{\mid\boldsymbol{r}-\boldsymbol{r}'\mid}. \quad (6)$$

Within the strong confinement limit, the depolarization tensors for the exciton and the biexciton have the same form, which is identical to that of a single exciton system [5]. In our numerical calculation of the PE spectrum, we use the experimentally estimated value of the depolarization shift for the exciton, which is given by $\Delta\omega_X = N_{xx}\mu_X^2/\hbar\epsilon_h V$, and expect the amount of the depolarization shift for the biexciton $\Delta\omega_B = N_{xx}\mu_B^2/\hbar\epsilon_h V$ using the ratio of the dipole moments between the exciton and the biexciton. Therefore, we need not estimate the detailed wave functions of the exciton and the biexciton, theoretically. We note, here, that the magnitude of the actual tensor for the biexciton is slightly greater than that of the exciton, because $\boldsymbol{p}_B(\boldsymbol{r})$ is more tightly localized to the center of a QD than $\boldsymbol{p}_X(\boldsymbol{r})$ [30].

For the derivation of the optical Bloch equations (OBEs) for the LFE including the biexciton, we use the noninteraction Hamiltonian,

$$H_0 = E_G|G\rangle\langle G| + E_X|X\rangle\langle X| + E_B|B\rangle\langle B|, \quad (7)$$

and the transition energies without the LFE, as $\hbar\omega'_B = E_B - E_X$ for the biexciton and $\hbar\omega'_X = E_X - E_G$ for the exciton. The interaction Hamiltonian between the external applied field $\boldsymbol{E}_{\rm ex}(\boldsymbol{r})$ and the polarization is

$$H_I = -\int d\boldsymbol{r}\hat{\boldsymbol{p}}(\boldsymbol{r})\cdot\boldsymbol{E}_{\rm ex}(\boldsymbol{r}). \quad (8)$$

The external applied field polarized along the x axis has the form

$$E_{\rm ex}(t) = \tfrac{1}{2}[\tilde{E}(t)e^{-i\omega t} + \tilde{E}^*(t)e^{i\omega t}], \quad (9)$$

where

$$\tilde{E}(t) = E(t)e^{i\boldsymbol{k}\cdot\boldsymbol{r}}, \quad (10)$$

and $E(t)$ represents an envelope function of the external applied electric field. The time evolution of the density matrix can be calculated by the relation

$$i\hbar\frac{\partial\rho}{\partial t} = [H_0 + H_I + H_{\rm dep}, \rho]. \quad (11)$$

By applying the rotating wave approximation, as $\tilde{\rho}_{BX} = \rho_{BX}e^{i\omega t}$, $\tilde{\rho}_{XG} = \rho_{XG}e^{i\omega t}$, and $\tilde{\rho}_{BG} = \rho_{BG}e^{2i\omega t}$, we obtain the OBEs, as

$$\frac{\partial\rho_{GG}}{\partial t} = i\frac{\mu_X\tilde{E}^*(t)}{2\hbar}\tilde{\rho}_{XG} - i\frac{\mu_X\tilde{E}(t)}{2\hbar}\tilde{\rho}^*_{XG} - i\Delta\omega_B^{0.5}\Delta\omega_X^{0.5}(\tilde{\rho}^*_{BX}\tilde{\rho}_{XG} - \tilde{\rho}_{BX}\tilde{\rho}^*_{XG}) + \frac{1}{T_1^X}\rho_{XX}, \quad (12)$$

$$\frac{\partial\rho_{XX}}{\partial t} = -i\frac{\mu_X\tilde{E}^*(t)}{2\hbar}\tilde{\rho}_{XG} + i\frac{\mu_X\tilde{E}(t)}{2\hbar}\tilde{\rho}^*_{XG} + i\frac{\mu_B\tilde{E}^*(t)}{2\hbar}\tilde{\rho}_{BX} - i\frac{\mu_B\tilde{E}(t)}{2\hbar}\tilde{\rho}^*_{BX} + 2i\Delta\omega_B^{0.5}\Delta\omega_X^{0.5}(\tilde{\rho}^*_{BX}\tilde{\rho}_{XG} - \tilde{\rho}_{BX}\tilde{\rho}^*_{XG}) + \frac{1}{T_1^B}\rho_{BB} - \frac{1}{T_1^X}\rho_{XX}, \quad (13)$$

$$\frac{\partial \rho_{BB}}{\partial t} = -i\frac{\mu_B \tilde{E}^*(t)}{2\hbar}\tilde{\rho}_{BX} + i\frac{\mu_B \tilde{E}(t)}{2\hbar}\tilde{\rho}^*_{BX} - i\Delta\omega_B^{0.5}\Delta\omega_X^{0.5}(\tilde{\rho}^*_{BX}\tilde{\rho}_{XG} - \tilde{\rho}_{BX}\tilde{\rho}^*_{XG}) - \frac{1}{T_1^B}\rho_{BB}, \quad (14)$$

$$\frac{\partial \tilde{\rho}_{XG}}{\partial t} = -i\{\omega'_X - \Delta\omega_X(\rho_{XX} - \rho_{GG}) - \omega\}\tilde{\rho}_{XG} - i\left(\frac{\mu_X \tilde{E}(t)}{2\hbar} - \Delta\omega_B^{0.5}\Delta\omega_X^{0.5}\tilde{\rho}_{BX}\right)(\rho_{XX} - \rho_{GG}) + i\left(\frac{\mu_B \tilde{E}^*(t)}{2\hbar} - \Delta\omega_B^{0.5}\Delta\omega_X^{0.5}\tilde{\rho}^*_{XG} - \Delta\omega_B\tilde{\rho}^*_{BX}\right) \times\tilde{\rho}_{BG} - \frac{1}{T_2^X}\tilde{\rho}_{XG}, \quad (15)$$

$$\frac{\partial \tilde{\rho}_{BG}}{\partial t} = -i(\omega'_X + \omega'_B - 2\omega)\tilde{\rho}_{BG} + i\frac{\mu_B \tilde{E}(t)}{2\hbar}\tilde{\rho}_{XG} - i\frac{\mu_X \tilde{E}(t)}{2\hbar}\tilde{\rho}_{BX} - i(\Delta\omega_B - \Delta\omega_X)\tilde{\rho}_{BX}\tilde{\rho}_{XG} + i\Delta\omega_B^{0.5}\Delta\omega_X^{0.5}\left(\tilde{\rho}^2_{BX} - \tilde{\rho}^2_{XG}\right) - \frac{1}{T_2^{BG}}\tilde{\rho}_{BG}, \quad (16)$$

$$\frac{\partial \tilde{\rho}_{BX}}{\partial t} = -i\{\omega'_B - \Delta\omega_B(\rho_{BB} - \rho_{XX}) - \omega\}\tilde{\rho}_{BX} - i\left(\frac{\mu_B \tilde{E}(t)}{2\hbar} - \Delta\omega_B^{0.5}\Delta\omega_X^{0.5}\tilde{\rho}_{XG}\right) \times(\rho_{BB} - \rho_{XX}) - i\left(\frac{\mu_X \tilde{E}^*(t)}{2\hbar} - \Delta\omega_X\tilde{\rho}^*_{XG} - \Delta\omega_B^{0.5}\Delta\omega_X^{0.5}\tilde{\rho}^*_{BX}\right) \times\tilde{\rho}_{BG} - \frac{1}{T_2^B}\tilde{\rho}_{BX}. \quad (17)$$

Here, we added the phenomenological damping terms of the exciton lifetime T_1^X, the biexciton lifetime T_1^B, the exciton dephasing time T_2^X, the biexciton dephasing time T_2^B, and the two-photon coherence time between the biexciton and the ground state T_2^{BG}. As can been seen in Eqs. (15) and (17), in the LFE, the transition frequencies of the biexciton and the exciton depend on the population difference as $\omega_B = \omega'_B - \Delta\omega_B(\rho_{BB} - \rho_{XX})$ and $\omega_X = \omega'_X - \Delta\omega_X(\rho_{XX} - \rho_{GG})$, respectively. The terms with a coefficient of $\Delta\omega_B^{0.5}\Delta\omega_X^{0.5} = N_{xx}\mu_B\mu_X/\hbar\epsilon_h V$ arise from the interaction between the depolarization field induced by the B-X transition and the polarization given by the X-G transition, and between the X-G depolarization field and the B-X polarization. These terms oscillate with a frequency of $\sim\Delta E_B/\hbar$, contributing little to the optical response.

The numerical calculation was performed as follows. In our measurement, the monochromator with a narrow entrance slit spatially extracted an approximately one-dimensional component from the focused image of the signal on the slit. Therefore, in the calculation, we treat a one-dimensional QD array system, to take into account the spatial distribution of the excitation intensity arising from the Gaussian beam profile, which modifies the coherent optical properties of the QD ensemble [33]. The inhomogeneous broadening of the QD array was set to be wider than the laser spectrum. We numerically and nonperturbatively calculated the time evolution of each QD, which obeys the OBEs, when we irradiated the QD array with two excitation pulses with $\boldsymbol{k}_{1,2}$, and pulse areas $\theta_{1,2}$ dependent on the location in the beam spot. The PE spectrum was obtained by a Fourier transformation of the macroscopic polarization calculated as a function of time, which generates the PE signal along $2\boldsymbol{k}_2 - \boldsymbol{k}_1$. We estimated the relation between $I_{1,2}$ and the corresponding $\theta_{1,2}$ using $\mu_X = 15\,\mathrm{D}$ estimated from the Rabi oscillations in our previous report [6], which used the same sample and experimental setup except for the laser pulse duration. We evaluated the field amplitude of the excitation pulses using a refractive index of GaAs ($n_{\mathrm{GaAs}} = 3.6$) by assuming a hyperbaric secant pulse with a temporal duration of 120 fs, and obtained $\theta_1 \sim 0.7\pi$ and $\theta_2 \sim 0.4\pi$ at the beam center. We used $\Delta E_B = 2.3\,\mathrm{meV}$, and introduced the biexciton inhomogeneous linewidth of $\hbar\delta\omega_B = 0.5\,\mathrm{meV}$, which arises from inhomogeneity of the QDs [9]. The exciton and biexciton dephasing times were set to be the experimentally measured dephasing time at the dip position in the PE spectrum, as $T_2^X = 380\,\mathrm{ps}$ and $T_2^B = 380\,\mathrm{ps}$, respectively, and the exciton lifetime was $T_1^X = 2.0\,\mathrm{ns}$ [6]. We assumed a two-photon coherence time $T_2^{BG} = 190\,\mathrm{ps}$, and a biexciton lifetime $T_1^B = 1.3\,\mathrm{ns}$, which was decided by the ratio of the exciton and biexciton lifetimes reported in the literature [34,35]. We set the depolarization shift $\hbar\Delta\omega_X = 22\,\mu\mathrm{eV}$, which was experimentally obtained in our previous report [6]. The assumption of $T_1^B = 1.3\,\mathrm{ns}$ gives $\mu_B = 18.6\,\mathrm{D}$, which yields $\hbar\Delta\omega_B = 33\,\mu\mathrm{eV}$, when N_{xx} for the biexciton is identical to that of the exciton.

Figure 2(c) shows the calculated PE spectrum change. Photon energy zero is given by the center of the laser spectrum. The calculated spectrum, as a whole, qualitatively reproduces the observation. We also calculated the PE spectrum using several values of $\Delta\omega_B$ and T_2^{BG} in the ranges of $\Delta\omega_B/\Delta\omega_X = 1 \sim 2$ and $T_2^{BG}/T_2^B = 0.5 \sim 2$. The calculated spectra were not so sensitive to those values, indicating that the depolarization field induced by the B-X transition is essential to the observation. In the case of zero $\hbar\Delta\omega_B$, although the spectrum peak was slightly shifted to a lower energy, a double-peaked structure like the observation was not reproduced, as can be seen in Fig. 2(d), which also supports the importance of the B-X depolarization field for the observation.

Next, we qualitatively discuss the PE spectrum change. In a PE process, when the polarization excited by the first pulse at $t = 0$ oscillates as $\propto \exp(-i\omega_1 t)$ with the resonant frequency ω_1 during $0 < t < \tau$, the polarization giving the PE signal after the time-reversal process of the second pulse at $t = \tau$ can be written as $P_{\mathrm{PE}}(t) \propto \exp[-i\omega_2(t-\tau) + i\omega_1\tau]$ using the resonant frequency ω_2 during $t > \tau$. In two-level systems, because $\omega_2 = \omega_1$, all the polarizations completely rephase at $t = 2\tau$, giving a PE signal [36,37]. On the other hand, in the LFE, the second pulse changes the population differences as $\Delta\rho_D^{BX} = \rho_D^{BX}(t > \tau) - \rho_D^{BX}(t < \tau)$ and $\Delta\rho_D^{XG} = \rho_D^{XG}(t > \tau) - \rho_D^{XG}(t < \tau)$, where $\rho_D^{BX} = \rho_{BB} - \rho_{XX}$ and $\rho_D^{XG} = \rho_{XX} - \rho_{GG}$. The changes in the populations give different resonant frequencies to $\omega_{1,2}$, and yield phase differences $\omega_1\tau - \omega_2\tau = \Delta\omega_B\Delta\rho_D^{BX}\tau$ for the B-X polarization and

$\omega_1\tau - \omega_2\tau = \Delta\omega_X \Delta\rho_D^{XG}\tau$ for the X-G polarization at $t = 2\tau$. Therefore, larger $\Delta\rho_D^{BX}$ and $\Delta\rho_D^{XG}$ induced by the higher excitation regime, such as the centers of the laser spectrum and the beam spot, cause larger phase differences at $t = 2\tau$, which disturbs the rephasing and gives a weaker PE intensity around the high excitation regime. In our experiment measuring the spatially integrated and spectrally resolved signal, therefore, we observe the weaker PE intensity as a dip structure in the spectrum. Because the phase difference increases with τ, the dip is deeper with increasing τ. In addition, at the center of the laser spectrum, the exciton is highly populated, which effectively creates the biexciton from the exciton at the spectrum center. The B-X transition energy is smaller than the X-G transition. Therefore, the number of the polarizations giving the PE signal at low energy is larger than that at high energy, which shifts the PE spectrum to lower energy at $\tau = 50$ and 100 ps and gives higher signal intensity to the lower peak at $\tau = 200$ and 400 ps.

In the calculation, we set $T_2^{X,B} = 380$ ps, the same as the dephasing time at the dip in the PE spectrum, though the peak position shows $T_2 \sim 1$ ns. Therefore, the actual values of $T_2^{X,B}$ are larger than those of the calculation. The difference originates from the lack of the distributions of $\Delta\omega_{X,B}$ in the calculation. The distributions more effectively disturb the rephasing of the polarizations at $t = 2\tau$ at the spectrum center, and the PE response at the dip shows a faster decay even for large T_2. On the other hand, large T_2 increases the decay time at the peak. Therefore, we expect that the PE spectrum can be reproduced quantitatively as well as qualitatively by introducing the distributions. We also mention the relevance of our results to excitation induced dephasing (EID) [38,39]. To reproduce the PE spectrum by EID, the ratio of the excitation laser intensities between the dip and peak positions in the PE spectrum requires that T_2 increases three times for a decrease of the excitation intensity by one half. However, we confirmed that T_2 was not so sensitive to the excitation.

Next, we discuss the relevance to the electron-hole exchange interaction. $H_{\rm dep}$ in Eq. (1) is equivalent to the Hamiltonian describing the electron-hole exchange interaction [25–29]. For the theoretical treatment of electron-hole exchange interaction, $H_{\rm dep}$ is interpreted as a static Coulomb interaction between the photoinduced charge densities, i.e., $\rho(\boldsymbol{r}) = -\nabla \cdot \boldsymbol{p}(\boldsymbol{r})$, when one electron-hole pair is created in a QD. Therefore, the energy structure obtained by diagonalizing $H_0 + H_{\rm dep}$ provides a good description of the static optical properties of the QD, such as the exciton doublet structure seen in a single QD PL spectrum [28], which is usually measured by a nonresonant excitation of the upper quantum states by a cw laser [2]. On the other hand, our transient experiment performed by a resonant pulsed excitation directly probes a dynamic change in the polarization, leading to a clear observation of the other physical aspect of $H_{\rm dep}$ given by a change in the polarization, i.e., the LFE arising from the interaction between the polarization and the depolarization field.

Finally, aside from QDs, we expect that optically induced polarizations and associated depolarization fields will have an important effect in other quantum systems of size much smaller than the resonant wavelength. The depolarization field renormalizes the resonant frequency, which depends on the population difference between the quantum states inducing the polarization. The renormalization of the resonant frequency gives characteristic temporal optical properties, when the depolarization shift is greater than the homogeneous linewidth, i.e., $\Delta\omega > 1/T_2$, because the time evolution of the polarization is strongly affected by the resonant frequency shift, as can be seen in Eqs. (15) and (17).

IV. CONCLUSION

In conclusion, we observed a change in the PE spectrum in the InAlGaAs/AlGaAs QDs. The spectrum change could be systematically reproduced by numerical calculations, which introduced a depolarization field induced by the B-X transition to a conventional LFE for single excitons. Our results indicate the importance of depolarized fields in determining the optical properties of tightly localized systems.

ACKNOWLEDGMENTS

This paper was supported in part by Japan Society for the Promotion of Science KAKENHI Grants No. JP20740168 and No. JP23340083. We are grateful to A. Oiwa of Osaka University for the fabrication of the aperture on the sample. We thank Y. Ogawa of Joetsu University of Education, M. Sadgrove of Tohoku University, H. Ajiki of Tokyo Denki University, and M. Bamba of Osaka University for helpful discussions. Y.M. acknowledges support from the M. Ishida foundation.

[1] C. Kittel, *Introduction to Solid State Physics* (Wiley, New York, 1996).

[2] D. Gammon, E. S. Snow, B. V. Shanabrook, D. S. Katzer, and D. Park, Phys. Rev. Lett. **76**, 3005 (1996).

[3] G. Y. Slepyan, S. A. Maksimenko, A. Hoffmann, and D. Bimberg, Phys. Rev. A **66**, 063804 (2002).

[4] G. Y. Slepyan, A. Magyarov, S. A. Maksimenko, A. Hoffmann, and D. Bimberg, Phys. Rev. B **70**, 045320 (2004).

[5] G. Y. Slepyan, A. Magyarov, S. A. Maksimenko, and A. Hoffmann, Phys. Rev. B **76**, 195328 (2007).

[6] K. Asakura, Y. Mitsumori, H. Kosaka, K. Edamatsu, K. Akahane, N. Yamamoto, M. Sasaki, and N. Ohtani, Phys. Rev. B **87**, 241301 (2013).

[7] Y. Mitsumori, T. Watanuki, Y. Sato, K. Edamatsu, K. Akahane, and N. Yamamoto, Phys. Rev. B **95**, 155301 (2017).

[8] P. Borri, W. Langbein, S. Schneider, U. Woggon, R. L. Sellin, D. Ouyang, and D. Bimberg, Phys. Rev. Lett. **87**, 157401 (2001).

[9] H. Tahara, Y. Ogawa, F. Minami, K. Akahane, and M. Sasaki, Phys. Rev. Lett. **112**, 147404 (2014).

[10] T. Suzuki, R. Singh, M. Bayer, A. Ludwig, A. D. Wieck, and S. T. Cundiff, Phys. Rev. Lett. **117**, 157402 (2016).

[11] E. Mayer, G. Smith, V. Heuckeroth, J. Kuhl, K. Bott, A. Schulze, T. Meier, D. Bennhardt, S. Koch, P. Thomas *et al.*, Phys. Rev. B **50**, 14730 (1994).

[12] E. J. Mayer, G. O. Smith, V. Heuckeroth, J. Kuhl, K. Bott, A. Schulze, T. Meier, S. W. Koch, P. Thomas, R. Hey *et al.*, Phys. Rev. B **51**, 10909 (1995).
[13] T. F. Albrecht, K. Bott, T. Meier, A. Schulze, M. Koch, S. T. Cundiff, J. Feldmann, W. Stolz, P. Thomas, S. W. Koch *et al.*, Phys. Rev. B **54**, 4436 (1996).
[14] I. Abram and A. Maruani, Phys. Rev. B **26**, 4759 (1982).
[15] I. Abram, Phys. Rev. B **28**, 4433 (1983).
[16] C. C. Sung and C. M. Bowden, Phys. Rev. A **29**, 1957 (1984).
[17] R. Sauer, Phys. Rev. Lett. **31**, 376 (1973).
[18] G. Moody, R. Singh, H. Li, I. A. Akimov, M. Bayer, D. Reuter, A. D. Wieck, and S. T. Cundiff, Phys. Rev. B **87**, 045313 (2013).
[19] P. C. Becker, H. L. Fragnito, C. H. Brito Cruz, R. L. Fork, J. E. Cunningham, J. E. Henry, and C. V. Shank, Phys. Rev. Lett. **61**, 1647 (1988).
[20] R. G. Neuhauser, K. T. Shimizu, W. K. Woo, S. A. Empedocles, and M. G. Bawendi, Phys. Rev. Lett. **85**, 3301 (2000).
[21] H. D. Robinson and B. B. Goldberg, Phys. Rev. B **61**, R5086 (2000).
[22] P. G. Blome, M. Wenderoth, M. Hübner, R. G. Ulbrich, J. Porsche, and F. Scholz, Phys. Rev. B **61**, 8382 (2000).
[23] J. Seufert, R. Weigand, G. Bacher, T. Kümmell, A. Forchel, K. Leonardi, and D. Hommel, Appl. Phys. Lett. **76**, 1872 (2000).
[24] D. Birkedal, K. Leosson, and J. M. Hvam, Phys. Rev. Lett. **87**, 227401 (2001).
[25] H. Ajiki and K. Cho, Phys. Rev. B **62**, 7402 (2000).
[26] H. Ajiki, T. Tsuji, K. Kawano, and K. Cho, Phys. Rev. B **66**, 245322 (2002).
[27] T. Takagahara, Phys. Rev. B **47**, 4569 (1993).
[28] T. Takagahara, Phys. Rev. B **62**, 16840 (2000).
[29] K. Cho, *Optical Response of Nanostructures* (Springer-Verlag, Berlin, 2003).
[30] K. Matsuda, T. Saiki, S. Nomura, M. Mihara, Y. Aoyagi, S. Nair, and T. Takagahara, Phys. Rev. Lett. **91**, 177401 (2003).
[31] Y. Z. Hu, M. Lindberg, and S. W. Koch, Phys. Rev. B **42**, 1713 (1990).
[32] S. V. Nair and T. Takagahara, Phys. Rev. B **55**, 5153 (1997).
[33] M. Kujiraoka, J. Ishi-Hayase, K. Akahane, N. Yamamoto, K. Ema, and M. Sasaki, Phys. Status Solidi A **206**, 952 (2009).
[34] C. Santori, G. S. Solomon, M. Pelton, and Y. Yamamoto, Phys. Rev. B **65**, 073310 (2002).
[35] M. Wimmer, S. V. Nair, and J. Shumway, Phys. Rev. B **73**, 165305 (2006).
[36] L. Allen and J. H. Eberly, *Optical Resonance and Two Level Atoms* (Wiley, New York, 1975).
[37] T. Yajima and Y. Taira, J. Phys. Soc. Jpn. **47**, 1620 (1979).
[38] H. Wang, K. Ferrio, D. G. Steel, Y. Z. Hu, R. Binder, and S. W. Koch, Phys. Rev. Lett. **71**, 1261 (1993).
[39] H. Wang, K. B. Ferrio, D. G. Steel, P. R. Berman, Y. Z. Hu, R. Binder, and S. W. Koch, Phys. Rev. A **49**, R1551 (1994).